ECS Journal of Solid State Science and Technology, **3** (7) Q142-Q145 (2014)
2162-8769/2014/3(7)/Q142/4/$31.00 © The Electrochemical Society

Improved Cleaning Process for Textured ∼25 μm Flexible Mono-Crystalline Silicon Heterojunction Solar Cells with Metal Backing

Sayan Saha,[a,z] Mohamed M. Hilali,[a] Emmanuel U. Onyegam,[a] Sushant Sonde,[a] Rajesh A. Rao,[b] Leo Mathew,[b] Ajay Upadhyaya,[c] and Sanjay K. Banerjee[a]

[a]*Microelectronics Research Center, Department of Electrical and Computer Engineering, University of Texas, Austin, Texas 78758, USA*
[b]*Applied Novel Devices, Austin, Texas 78758, USA*
[c]*University Center of Excellence for Photovoltaics, Georgia Institute of Technology, Atlanta, Georgia 30332, USA*

An improved cleaning process is developed to remove front surface contamination for single heterojunction solar cells on textured surfaces on ∼25 μm thick exfoliated, flexible mono-crystalline silicon. The process is very effective in cleaning metallic and organic residues, without introducing additional contamination or degrading the supporting back metal used for ultrathin substrate handling. Quantitative analysis of the Auger electron spectra shows significant potassium contamination reduction (∼0.89% atomic) using the new cleaning process. An open-circuit voltage enhancement of 22 mV and an absolute 1.5% increase in conversion efficiency are observed with the new cleaning procedure for the exfoliated thin solar cells.

Manuscript submitted April 16, 2014; revised manuscript received May 22, 2014. Published May 30, 2014.

Thin crystalline silicon (c-Si) solar cells are of much interest due to their potential to achieve high efficiency and reduce cost by using less Si material. However, there are significant challenges to commercialize sub-100 μm thin Si substrates as they can easily break or crack with wafer-handling, resulting in low yield in a solar cell manufacturing line. We have introduced in our earlier work,[1] a kerf-less process in which ultra-thin (∼25 μm) and flexible mono-crystalline Si substrates can be obtained through an exfoliation technique from a thicker (>450 μm) parent wafer. These substrates, when exfoliated, have thick (∼50 μm) electroplated nickel (Ni) metal backing, which provides mechanical support to the thin Si and enables ease of processing for semiconductor device fabrication.

Previously we have demonstrated single heterojunction (SHJ) solar cells fabricated on this type of substrate exhibiting efficiencies 14.9% on as-exfoliated substrates.[2] However, on textured surfaces efficiency was limited to 11%. We postulated that one of the issues that could be limiting the performance of the cells is unintentional front surface contamination introduced during wet chemical processes before hydrogenated amorphous Si (a-Si:H) deposition of the front surface emitter, which can limit the open-circuit voltage (V_{OC}) of these solar cells. This could happen due to the presence of potassium ions introduced from potassium hydroxide (KOH) during texturing. For decontamination we could not use SC-2 solution (5:1:1 ratio of H_2O, H_2O_2, HCl at 80°C) as it reacts rather aggressively with the electroplated Ni back metal. Instead, we used a piranha solution (1:1 ratio of H_2O_2, H_2SO_4) for both decontamination from potassium ions and removal of organic contaminants, which did not seem to show corrosion degradation in the back side Ni. The pH level of HCl is slightly lower compared to H_2SO_4, and SC-2 solution has a stronger effervescent action than piranha solution. This may explain why the Ni is much more affected by the SC-2 clean compared to the piranha clean. Nevertheless, piranha-treatment alone is probably inadequate for metal residues or potassium related contaminant removal after texturing.

In this work, we attempted to address the front surface contamination issue by developing an improved cleaning procedure for textured silicon surfaces for mono-crystalline exfoliated Si substrate. We assumed the cleaning process employed for the rear surface is sufficient as it was done using traditional RCA cleaning[3] on a textured thick parent wafer. With the help of X-ray Photoelectron Spectroscopy (XPS) we have identified the chemical bonding nature of key contaminants at the surface i.e. carbon and potassium. We have also employed Auger electron spectroscopy (AES) to quantify the atomic concentration of the impurities before and after implementation of various wet chemical cleans. We have fabricated and characterized SHJ solar cells on both exfoliated and bulk (∼180 μm) substrates to study the effect of contamination on device performance and how an improved surface clean procedure can affect the solar cell efficiency.

Experimental

A detailed process flow for the exfoliation process is discussed in previous work.[4] For spectroscopic analysis, we cut exfoliated substrates into 10×10 mm^2 pieces. These small area substrates were degreased by using acetone and isopropyl alcohol (IPA) sonication. They were then textured on the front (exfoliated) side using a KOH (2%), IPA (8%) and water mixture at 80°C followed by a 5 minute deionized (DI) water rinse. Four separate samples (numbered 1 to 4) were fabricated based on the surface treatment they went through, right after texturing. Sample 1 is used as a control sample with no additional cleaning processes done to decontaminate the surface. Sample 2 was cleaned with piranha solution (1:1 ratio of H_2O_2, H_2SO_4) for 2 minutes. This is the old cleaning procedure employed in our previous work.[2] Sample 3 was treated with a 1:40 water based solution of SC-15[5] (Surface Chemistry Discoveries, Inc.) at 40°C for 5 minutes. SC-15 is used as an alternative to RCA clean. It is well documented in the literature[6,7] that SC-1 step (5:1:1 ratio of H_2O, H_2O_2, NH_4OH at 80°C) in RCA cleans causes micro-roughening and even pitting of silicon substrates, thereby introducing trap states (D_{it}) at the heterointerface.[8] We ensure extremely low anisotropic silicon etch rate to reduce roughening the surface by using high dilution (1:40) of SC-15 formulation. This is verified by scanning electron microscopy (SEM) done before and after SC-15 treatment. The surface morphology doesn't change as the solution was not concentrated enough and the temperature wasn't high enough to round off the peaks of the random pyramids that has been typically shown in previous literature[9,10] due to different isotropic etches for heterojunction cell processing. The diluted solution has a composition of 0.05 to 10% by weight water soluble alkanolamine, 0.01 to 2.5% by weight of quaternary ammonium hydroxide, 0.01 to 2% by weight chelating agent, and the pH of this composition is about 10 to 13. The solvating action of quaternary ammonium hydroxide helps in removing the organic compounds, and additionally raises the pH level to help the organic amine remove metal contaminants, which acts as a ligand and forms complexes with the metal cations.[11,12] The chelating agent was used to increase the capacity of the cleaning bath to retain metals in solution by acting as a multi-dentate ligand forming a stable multi-dentate complex with the metal cations, which enhances the dissolution of metallic residues on the silicon surface.[13,14] The temperature of 40°C aids in the contaminant removal, but is still not high enough to result in anisotropic etching of the silicon. Finally, sample 4 was treated

[z]E-mail: sayan.saha@utexas.edu

Table I Cleaning/etching processes used in preparing samples 1 to 4 for XPS and AES analysis.

Step	Sample 1	Sample 2	Sample 3	Sample 4
1	Acetone+IPA sonication	Acetone+IPA sonication	Acetone+IPA sonication	Acetone+IPA sonication
2	Texturing (2% KOH+ 8% IPA)	Texturing (2% KOH+ 8% IPA)	Texturing (2% KOH+ 8% IPA)	Texturing (2% KOH+ 8% IPA)
3	5 min DI water rinse	5 min DI water rinse	5 min DI water rinse	5 min DI water rinse
4	5% HF dewet	5% HF dewet	5% HF dewet	5% HF dewet
5	-	5 min DI water rinse	5 min DI water rinse	5 min DI water rinse
6	-	Piranha (2 min)	SC-15 (@40°C, 2 min)	SC-15 (@40°C, 2 min)
7	-	5 min DI water rinse	5 min DI water rinse	5 min DI water rinse
8	-	5% HF dewet	5% HF dewet	5% HF dewet
9	-	-	-	5 min DI water rinse
10	-	-	-	Piranha (2 min)
11	-	-	-	5 min DI water rinse
12	-	-	-	5% HF dewet

with SC-15, followed by DI water rinse and then 2 minute piranha cleaning process. This was done to see if additional piranha clean at the end results in further removal of organic impurities from the surface. Complete details of the cleaning steps employed on samples 1 to 4 are shown in Table I.

XPS measurements were carried out on these four samples using monochromatic Al Kα X-ray source of 1486.7 eV excitation energy with an analyzer work function of 4.5 eV. For this analysis we concentrated our focus on monitoring photoelectron peaks for organic (carbon) (C) and potassium (K). This was done based on the identification of probable organic/metallic contamination in the XPS survey spectra. High-resolution multi-region spectra of the main signals, i.e. C 1*s*, O 1*s* and K 2*p* with Gaussian-Lorentzian curve (continuous line) fitting of the recorded photoelectron spectra (points) was used in order to characterize and understand the chemical bonding nature of the contaminants based on the observed chemical shifts.

Samples 1 to 4 were also characterized using AES in situ. AES provides higher lateral resolution measurement when the surface distribution of the elements is less than a micrometer scale.[15] To detect trace amount of contaminants on a surface this might be useful. The AES peaks are superimposed on an imported background of different types of secondary electrons. Hence, the AES spectra are represented in the differentiated form. After differentiation the data is further smoothened using a five point Savitzky-Golay filter.

Single heterojunction cells with diffused back junction were fabricated to evaluate the efficacy of the developed new clean (sample 4) as compared to the old clean (sample 2) on exfoliated substrates with front-surface texture. The thickness of the Indium Tin Oxide (ITO) is reduced from 100 nm (used in previous work[2]) to 75 nm to increase short wavelength response. Current-voltage (J-V) measurements were carried out to obtain the short-circuit current density (J_{SC}), open-circuit voltage (V_{OC}), and maximum power point (MPP) for cells that employed the old cleaning process, and the new cleaning process, under AM 1.5 sun illumination. The measurement was done using a 1.1 cm^2 cell aperture area. Internal quantum efficiency (IQE) measurements (Figure 4b) for the individual cells were calculated from corresponding external quantum efficiency (EQE) and reflectance (R) measurement data (IQE = EQE/(1-R)) to obtain a more accurate representation of the spectral collection efficiency. We have also fabricated ~180 μm thick wafer-based solar cells using identical process flow (save for the exfoliation step) and device architecture to that of the ultrathin solar cells. These cells are fabricated in order to compare their performance to that of the exfoliated solar cells. For this experiment we have compared samples which have gone through old (sample 2) and new (sample 4) cleaning procedure.

Results and Discussion

The C 1*s* (284.6 eV) and K 2*p* (292.9 eV) photoelectron peaks are very close to each other and the former is a more intense peak than the latter one, thereby making the K 2*p* peak less apparent in a survey spectra scan in Figure 1. In Figure 2a the main peak of

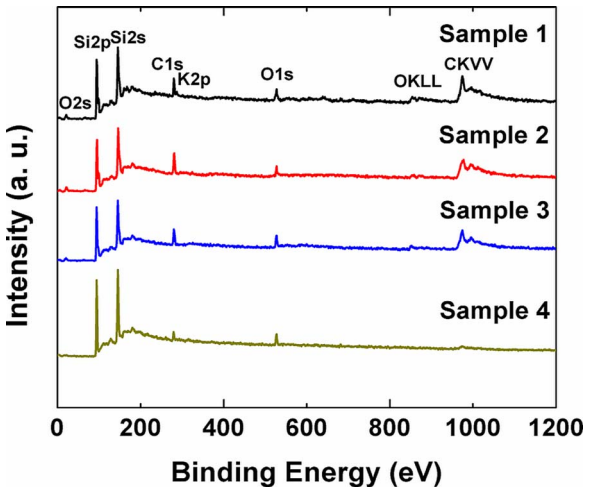

Figure 1. (Color online) XPS survey spectra of the different sample surfaces.

the C 1*s* signal at 284.6 eV is due to hydrocarbons. The other fitted peaks show binding energy signals due to different C-O functional groups.[16] The source for these C peaks in sample 1 could be due to trace amounts of IPA residue from the KOH solution, as well as dissociation of organic additives (brightener) and carbonate (used to

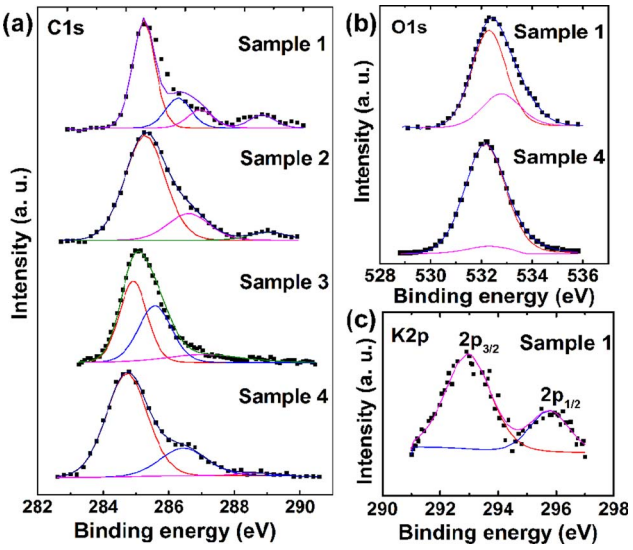

Figure 2. (Color online) XPS multi-region high-resolution spectra of different sample surfaces, showing photoelectron peaks with Gaussian-Lorentzian fitting. The intensity is shown with arbitrary units (a. u.).

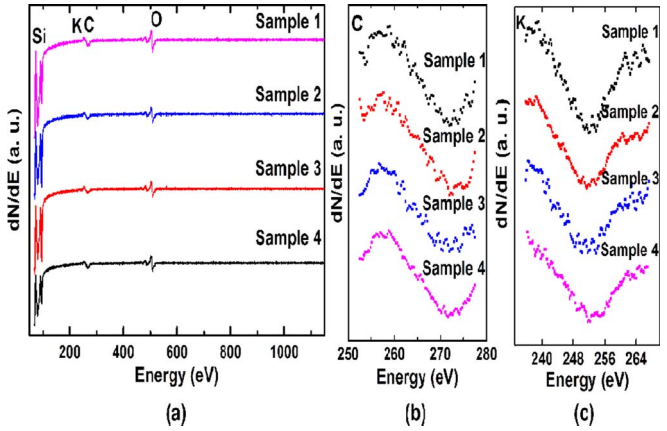

Figure 3. (Color online) (a) AES survey spectra of the different sample surfaces, (b) AES multi-region high-resolution spectra of different sample surfaces with differentiated peaks for C (272 eV) and (c) differentiated peaks for K (252 eV). The intensity is shown with arbitrary units (a. u.).

maintain pH balance of the electroplating bath) from the electroplated back metal. Some of these C-O peaks become relatively less intense or nonexistent compared to C-C peak in subsequent samples (2-4) with improved sample cleans. This effect is most prominent in sample 4. This suggests that the organic contamination is most effectively removed when the cleaning procedure in sample 4 is employed. This could be validated further by comparing the O 1*s* peak for the most contaminated sample (i.e. sample 1) with that of sample 4. When the O 1*s* peak is de-convoluted to find out the different contributions (Figure 2b), it shows peaks due to native oxide (SiO_x) at 532.2 eV and C-O bonding at 532.8 eV. In case of sample 4, the relative intensity of the peak suggesting C-O bonding is significantly less than that in sample 1. For sample 4 the peak due to SiO_x is more dominant, suggesting a surface less organically contaminated. For K $2p_{3/2}$ (292.9 eV), K $2p_{1/2}$ (295.7 eV) peaks, only sample 1 shows any detectable intensity (Figure 2c), even in high spatial resolution XPS (0.2 mm diameter lens aperture). This is probably due to limitation in lateral detection area posed due to high spatial resolution lens aperture compounded by non-uniform distribution of K contaminants. With 0.2 mm lens aperture the photoelectron counts for K is lost in the background noise for samples 2, 3 and 4.

Figure 3a shows the AES survey spectra of the substrate surfaces for the four samples. Figure 3b and 3c show high resolution spectra for C (272 eV) and K (252 eV) respectively. The concentration of each element is calculated by $C_X = \frac{\frac{I_X}{S_X d_X}}{\sum \frac{I_j}{S_j d_j}}$; where I_X is the peak-to-peak amplitude of the element X from the test spectra, S_X and d_X are the relative sensitivity and the scale factor of the element X, respectively; Σ denotes the sum for all the peaks.[17] Table II gives the atomic concentrations for C and K. The percentage data shown in Table II suggest that although the old clean (sample 2) reduces the C and K contamination by 0.52% and 0.23% absolute, respectively; SC-15 is much more effective in reducing the K contaminant (by 0.86% absolute), and organic contaminants are reduced by 0.73% absolute as observed for sample 3. Some heavy organic contaminants may be hard to oxidize and remove through piranha clean alone. However, a piranha clean following SC-15 is even more effective in reducing the organic contaminants further down by 0.48% from sample 3. Therefore, the cleaning process used in sample 4 is more optimal in reducing both C (by 1.21% absolute) and K (by 0.89% absolute) contamination.

Table III. J-V data summary at AM1.5 illumination for solar cells on exfoliated substrates, based on cleaning process employed.

Cell	V_{OC} (mV)	J_{SC} (mA/cm^2)	FF (%)	Efficiency (%)
old clean	525	35.2	64	11.8
new clean	547	35.9	67.5	13.3

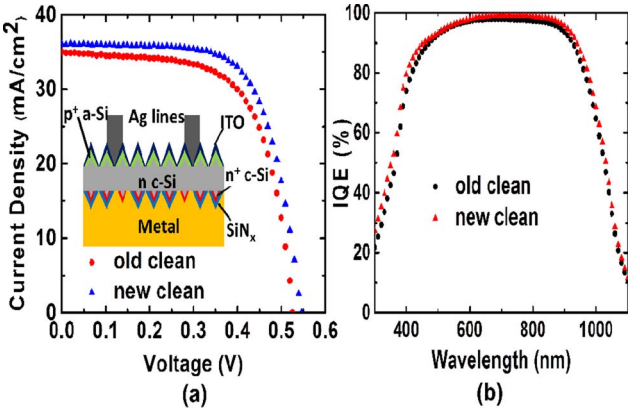

Figure 4. (Color online) (a) J-V characteristics at AM1.5 illumination for solar cells on exfoliated ~25 μm thick substrates, differentiated based on cleaning process employed (cell structure is shown inset), (b) IQE response measured on textured solar cells on exfoliated ~25 μm thick substrates in the 300–1100 nm range.

The current-voltage results for the exfoliated cells are summarized in Table III and the J-V curves are shown in Figure 4a. We observed that with the newer and more optimized cleaning process the V_{OC} increases by 22 mV, and the current increases by 0.7 mA/cm^2. The fill factor is further increased by 3.5% absolute. As a result the overall efficiency increases by 1.5% absolute (or 12.7% relative). This again indicates that the new cleaning process is more effective in removing elements that can result in mid-gap traps like potassium in Si. The solar cell with the new cleaning process shows an average of 4.5% improvement in short-wavelength response (300-500 nm) (Figure 4b), as compared to the cell using the old cleaning procedure. This suggests reduced surface recombination at the a-Si:H/c-Si interface due to reduction in surface states. The slight improvement in the mid-to-near infrared wavelength response suggests that bulk lifetime may have effectively been slightly improved as well for such ultrathin Si solar cell with the new clean compared to that using the old clean. However, in order to achieve a V_{OC} greater than 600 mV we still need to optimize the thin film deposition on textured surfaces and use intrinsic a-Si layer (i-layer) to passivate the dangling bonds at the c-Si surface.

The current-voltage results for the bulk cells are summarized in Table IV and the J-V curve is shown in Figure 5a. The corresponding IQE curves are shown in Figure 5b. The V_{OC} of the cell which has gone through new cleaning method is 9 mV higher and the overall efficiency is improved only by 0.45% absolute (or 3% relative). The 576 mV is comparable with the expected V_{OC} that is possible to achieve with no i-layer surface passivation.[18] The improvement in short-wavelength response, as shown in Figure 5b, is quite small. The reason that the improvement due to the new cleaning method is not as much as that

Table II. Atomic percentages calculated for C and K from the surfaces of samples 1 to 4.

Sample	Sample 1	Sample 2	Sample 3	Sample 4
C	2.84%	2.32%	2.11%	1.63%
K	1.11%	0.88%	0.25%	0.22%

Table IV. J-V data summary at AM1.5 illumination for solar cells on bulk substrates (~180 μm), based on cleaning process employed.

Cell	V_{OC} (mV)	J_{SC} (mA/cm^2)	FF (%)	Efficiency (%)
old clean	567	36.2	71.4	14.65
new clean	576	36.7	71.4	15.1

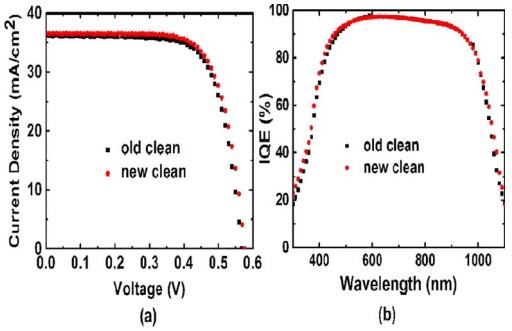

Figure 5. (Color online) (a) J-V characteristics at AM1.5 illumination for solar cells on exfoliated ∼180 μm thick substrates, differentiated based on cleaning process employed (cell structure is identical to that in Figure 4a), (b) IQE response measured on textured solar cells ∼180 μm thick substrates in the 300–1100 nm range.

observed on cells made on exfoliated substrates is because surface recombination is a more dominant factor affecting V_{OC} in case of the much thinner ∼25 μm thick substrates compared with the ∼180 μm thick substrate. Consequently, such thin substrates have a very stringent requirement for surface passivation to achieve high V_{OC}. Due to a more relaxed surface passivation requirement; cells made on a thicker bulk substrate tend to show higher V_{OC} for similar surface passivation.

The J-V and IQE characteristics shown for both exfoliated and bulk cells above are taken from a batch of four cells in each case. The average increment in efficiency is 1.35% and 0.36% for ∼25 μm and ∼180 μm cells respectively; the standard deviation of increment in efficiency is 0.12% and 0.09% respectively. The average and standard deviation statistics are shown for both exfoliated and bulk cells in Figure 6.

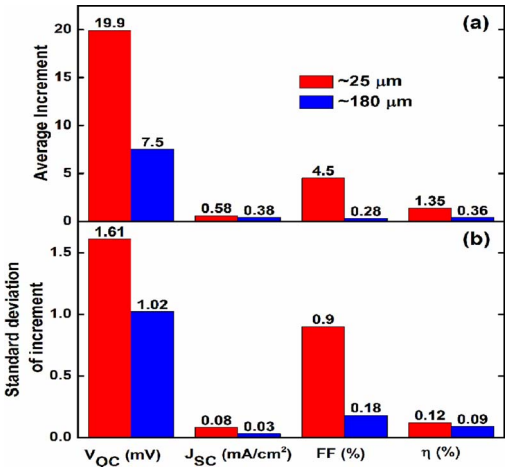

Figure 6. (Color online) (a) Comparison of average increment in V_{OC}, J_{SC}, FF and efficiency (η) between exfoliated (∼25 μm) and bulk (∼180 μm) cells, (b) Comparison of standard deviation of increment in V_{OC}, J_{SC}, FF and efficiency (η) between exfoliated (∼25 μm) and bulk (∼180 μm) cells.

Summary

In this work we have developed a cleaning process to effectively remove surface contamination on textured, exfoliated ∼25 μm thick substrates without degrading the back metal or introducing additional metallic or organic contamination. XPS measurements were carried out. Carbon and potassium were detected to be the main contaminants and their chemical bonding nature was evaluated. AES measurement was used to monitor the concentration changes on the surface following the different cleaning processes. Completed single heterojunction solar cells on ultrathin substrates with the new and improved cleaning process show a significant improvement in V_{OC} by 22 mV and an efficiency increase of 1.5% absolute.

Acknowledgments

We thank D. Jawarani, R. S. Smith and D. Xu for their contribution in developing exfoliation process. This work was supported in part by the Bay Area Photovoltaics Consortium (BAPVC) program under award number DE-EE0004946.

References

1. R. A. Rao et al., in *38th IEEE Photovoltaic Specialists Conference (PVSC)*, p. 1837–1840, Austin, TX (2012) http://ieeexplore.ieee.org/xpl/articleDetails.jsp?arnumber=6317951.
2. S. Saha et al., *Appl. Phys. Lett.*, **102**, 163904 (2013).
3. W. Kern, *J. Electrochem. Soc.*, **137**, 1887–1892 (1990).
4. D. Xu et al., in *IEEE International Reliability Physics Symposium (IRPS)*, p. 4A.3.1–4A.3.7, Anaheim, CA (2012).
5. S. Naghshineh, E. Oldak, and G. Schwartzkopf, (2012) http://www.freepatentsonline.com/20120187336.pdf.
6. H. F. Schmidt et al., *Jpn. J. Appl. Phys.*, **34**, 727–731 (1995) http://iopscience.iop.org/1347-4065/34/2S/727/pdf/1347-4065_34_2S_727.pdf.
7. S. Verhaverbeke et al., in *Electron Devices Meeting*, p. 71–74, Washington, DC (1991) http://ieeexplore.ieee.org/stamp/stamp.jsp?tp=&arnumber=235421.
8. W. G. J. H. M. van Sark, L. Korte, and F. Roca, F. Eds., *Physics and Technology of Amorphous-Crystalline Heterostructure Silicon Solar Cells*, 1st ed., Springer, Berlin, (2012), p. 45–94.
9. M. Edwards, S. Bowden, U. Das, and M. Burrows, *Sol. Energy Mater. Sol. Cells*, **92**, 1373–1377 (2008) http://linkinghub.elsevier.com/retrieve/pii/S0927024808001864.
10. L. Fesquet et al., in *34th IEEE Photovoltaic Specialists Conference (PVSC)*, p. 000754–000758, IEEE, Philadelphia, PA (2009).
11. K. A. Reinhardt and W. Kern, Eds., *Handbook of Silicon Wafer Cleaning Technology*, 2nd ed., William Andrew Inc., Norwich, (2008), p. 25, 28–29.
12. B. Kanegsberg and E. Kanegsberg, Eds., *Handbook for Critical Cleaning: Cleaning Agent and Systems*, 2nd ed., CRC Press, Boca Raton, (2011), p. 73–74.
13. C. Beaudry, H. Morinaga, and S. Verhaverbeke, in *Ceaning Technology in Semiconductor Device Manufacturing VII*, p. 118–125, Electrochemical Society Inc., Pennington (2002) http://www.electrochem.org/dl/ma/200/pdfs/1414.pdf.
14. G. W. Gale et al., *J. Electrochem. Soc.*, **148**, G513 (2001).
15. M. Prutton and M. M. El Gomati, Eds., *Scanning Auger Electron Microscopy*, 1st ed., John Wiley & Sons, Ltd, Chichester, UK, (2006), p. 3–12.
16. E. Desimoni, G. I. Casella, A. M. Salvi, T. R. I. Cataldi, and A. Morone, *Carbon N. Y.*, **30**, 527–531 (1992).
17. L. E. Davis, N. C. MacDonald, P. W. Palmberg, and G. E. Riach, *Handbook of Auger electron spectroscopy: A reference book of standard data for identification and interpretation of Auger electron spectroscopy data*, 2nd ed., Physical Electronics Industries, Eden Prairie, (1976), p. 5.
18. M. Taguchi, A. Terakawa, E. Maruyama, and M. Tanaka, *Prog. Photovoltaics Res. Appl.*, **13**, 481–488 (2005).